

Martensite transformation of epitaxial Ni–Ti films

J. Buschbeck, J. K. Kawasaki, A. Kozhanov, R. D. James, and C. J. Palmstrøm

Citation: *Applied Physics Letters* **98**, 191901 (2011); doi: 10.1063/1.3589361

View online: <http://dx.doi.org/10.1063/1.3589361>

View Table of Contents: <http://scitation.aip.org/content/aip/journal/apl/98/19?ver=pdfcov>

Published by the [AIP Publishing](#)

Articles you may be interested in

[Structural transformations in NiTi shape memory alloy nanowires](#)

J. Appl. Phys. **115**, 194307 (2014); 10.1063/1.4876715

[Growth of epitaxial NiTi shape memory alloy films on GaAs\(001\) and evidence of martensitic transformation](#)

J. Vac. Sci. Technol. B **29**, 03C116 (2011); 10.1116/1.3556973

[Thin film NiTi coatings on optical fiber Bragg sensors](#)

Appl. Phys. Lett. **93**, 031914 (2008); 10.1063/1.2961002

[Signature of martensite transformation on conductivity noise in thin films of NiTi shape memory alloys](#)

Appl. Phys. Lett. **92**, 112110 (2008); 10.1063/1.2896304

[Graphoepitaxial NiTi shape memory thin films on Si](#)

Appl. Phys. Lett. **73**, 750 (1998); 10.1063/1.121989



AIP | Journal of
Applied Physics

Journal of Applied Physics is pleased to
announce **André Anders** as its new Editor-in-Chief

Martensite transformation of epitaxial Ni–Ti films

J. Buschbeck,^{1,a)} J. K. Kawasaki,² A. Kozhanov,¹ R. D. James,³ and C. J. Palmström^{1,2}

¹Department Electrical and Computer Engineering, University of California, Santa Barbara, CA 93106 USA

²Department of Materials, University of California, Santa Barbara, CA 93106 USA

³Department of Aerospace Engineering and Mechanics, University of Minnesota, Minneapolis, MN 55455 USA

(Received 11 March 2011; accepted 18 April 2011; published online 10 May 2011)

The structure and phase transformations of thin Ni–Ti shape memory alloy films grown by molecular beam epitaxy are investigated for compositions from 43 to 56 at. % Ti. Despite the substrate constraint, temperature dependent x-ray diffraction and resistivity measurements reveal reversible, martensitic phase transformations. The results suggest that these occur by an in-plane shear which does not disturb the lattice coherence at interfaces. © 2011 American Institute of Physics. [doi:10.1063/1.3589361]

NiTi is arguably the most technologically important shape memory alloy.^{1,2} Its martensitic phase transformations have been widely studied in bulk³ and polycrystalline films.⁴ However, little work has been reported on epitaxial Ni–Ti films,⁵ whose transformation strains could even exceed those of polycrystalline films.⁶ In this letter, the structure and martensitic transformations of epitaxial Ni–Ti films are investigated.

Ni–Ti films were grown in a VG80 molecular beam epitaxy system at 5×10^{-10} mbar on MgO(001) substrates using codeposition of elemental Ni and Ti from effusion cells. The film composition was set by adjusting the cell temperatures to achieve the desired Ni/Ti flux ratio. Since it was found that the B2 order in the films improves with substrate temperature, growth was performed at highest temperature of 700 °C. The films were grown to a thickness of 35 ± 2 nm at an average growth rate of 11 nm/h. The film composition and thickness were determined by Rutherford backscattering spectrometry. X-ray diffraction (XRD) measurements were performed using Cu K α radiation. For temperature dependent XRD, the samples were mounted onto a thermoelectric cooler with a temperature range from 260 to 365 K. Temperature dependent electrical resistivity was measured in 4-contact geometry in a Quantum Design Physical Property Measurement System.

Room temperature (RT) XRD θ - 2θ scans on Ni–Ti films with different composition are shown in Fig. 1. All films exhibit prominent intensity peaks close to the (001) and (002) reflection positions of the bulk NiTi B2 austenite ($a=0.3015$ nm, Ref. 3). For films with ≤ 50 at. % Ti, these are single-peaks that can be ascribed to an B2 ordered austenitic phase. An XRD pole figure measurement of the B2{101} reflections [Fig. 1(b)] shows that the epitaxial orientation relationship is as follows: NiTi-B2(001)[110]||MgO(001)[100] [Fig. 1(c)]. Due to the lattice mismatch $f=(a_{\text{MgO}}-\sqrt{(2)a_{\text{B2}}})/a_{\text{MgO}}=-1.3\%$, compressing the film lattice in the plane, the NiTi B2 structure grows tetragonally distorted with an expanded out-of-plane lattice parameter, resulting in a peak shift to smaller angles as compared to the positions expected for bulk B2(00L). On

films with ≤ 47 at. % Ti an additional peak at 74.2° is detected, which is close to the expected (220) reflection of Ni₃Ti (Ref. 3). Films with Ti contents ≥ 51 at. %, exhibit double-peaks at the B2(00L) reflection positions.

Since the occurrence of double peaks in XRD can indicate martensite formation,⁷ the films were investigated for structural transformations by measuring temperature dependent θ - 2θ scans around the B2(002) position (Fig. 2). Consistent with Fig. 1(a), for stoichiometric composition [Fig. 2(a)] a single peak ($2\theta \sim 60.5^\circ$) is observed at RT and above, which is associated with the B2 austenite phase. Upon cooling, this peak shifts to a slightly lower angle and decreases in intensity. The formation of an additional diffraction peak at $T < 285$ K ($2\theta \sim 61^\circ$) marks the beginning of a martensite phase formation. By heating up to 299 K again, the film transforms back to the austenite (single peak at $2\theta \sim 60.5^\circ$). Figure 2(b) shows for a Ti-rich sample (51 at. %Ti) that the double peak that was observed at RT [Fig. 1(a)] vanishes upon heating and the B2 phase ($2\theta \sim 60.5^\circ$) forms at 318 K and above. Upon subsequent cooling from 343 K to 310 K, first the intensity of the B2(002) diffraction peak decreases and similar to Fig. 2(a), a peak forms at $2\theta \sim 61^\circ$. When

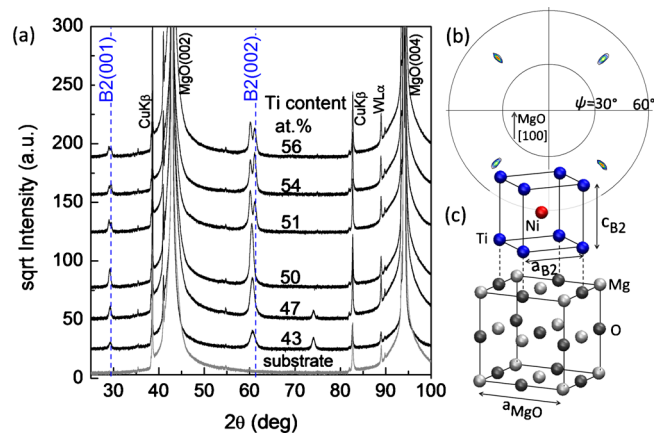


FIG. 1. (Color online) (a) XRD θ - 2θ scans of epitaxial Ni–Ti/MgO(001) heterostructures with different Ti contents at RT. Dashed lines mark the (00L) reflection positions of bulk NiTi B2. (b) B2{101} pole figure of the Ni₅₀Ti₅₀ film with MgO[100] substrate direction shown by an arrow. (c) Schematic of the epitaxial orientation relationship of NiTi B2 on MgO(100).

^{a)}Electronic mail: jbuschbeck@ece.ucsb.edu.

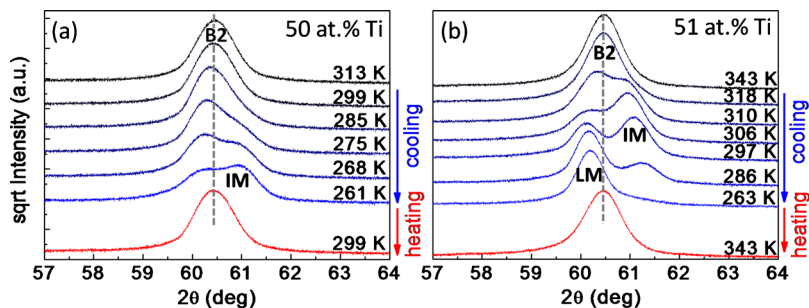


FIG. 2. (Color online) XRD θ - 2θ scans measured on $\text{Ni}_{50}\text{Ti}_{50}$ and $\text{Ni}_{49}\text{Ti}_{51}$ films near $B2(002)$ in several temperature steps during cooling and after heating up again. Reflections of the individual phases are labeled.

cooling further to below 306 K, another peak forms at $2\theta \sim 60^\circ$ which finally becomes the only observable peak at 263 K. This sequence of peaks is interpreted as $B2$ first transforming into an intermediate martensite (IM), followed by the transformation into a second, low temperature martensite (LM). By subsequently heating to 343 K, the $B2$ austenite is recovered with no evidence for the reformation of IM, indicating that this phase is metastable. The coexistence of LM and IM explains the double-peaks observed in XRD on Ti-rich samples at RT [Fig. 1(a)].

Further information about these transformations was obtained from temperature dependent reciprocal space maps (RSMs). Measurements of the normal lattice spacings were performed along $B2[110]$, around the $B2(002)$ reflection [Fig. 3(a)]. The RSMs show that the peak intensities of $B2$ and IM as well as LM line up along $B2[001]$. This perpendicular alignment signifies that change in the out-of-plane lattice spacing does not involve tilting of the lattice planes. Measurements along $B2[100]$ lead to the identical result. RSMs were also measured around the inclined $B2(011)$ plane in a measurement plane spanned by $B2[100]$ and $B2[011]$ [Fig. 3(b)]. Symmetric peak splitting along $B2[011]$ is observed upon transformation $B2 \rightarrow IM$. This geometry is consistent with formation of two oppositely sheared variants of the IM phase [one is schematically illustrated in Fig. 3(b)]. By symmetry, four such variants are expected. The reflections of the “missing” two variants however are lying out of the measurement plane and hence are not observed. Upon further cooling the intensities vanish, suggesting that the reciprocal lattice spots of LM are not lying in the measurement plane.

In order to investigate a wider temperature range, resistivity measurements were performed during cooling and heating [Fig. 4(a)]. Hysteretic behavior is observed for all compositions. Upon cooling from the $B2$ phase, a departure from linearity and increase in resistivity marks the start of the IM formation. This behavior is interpreted to result from electron scattering at phase boundaries during the phase transition. A maximum in resistivity is observed when IM and LM coexist while the formation of single phase LM at the lowest temperatures results in a linear behavior. Upon heating, no indication of an IM formation is observed, which is in agreement with the XRD measurements. Only a weak increase in resistivity occurs when LM and austenite coexist. From the measurement curves, the transformation start temperatures (IM_S and LM_S) were estimated by linear extrapolation and by the maximum in resistivity, respectively, as shown in Fig. 4(a) for a film with 56 at. % Ti. It is observed that LM_S decreases with decreasing Ti content while IM_S exhibits little variation [Fig. 4(b)]. For some compositions, IM_S and LM_S were verified by XRD using the first appearance of the respective reflection of IM and LM (open symbols).

For Heusler shape memory alloys it was reported that the substrate clamping completely suppresses martensitic transformations in 90 nm thick epitaxial films.⁸ Hence it is surprising that martensitic phase transformations are observed in the present 35 nm thin epitaxial Ni-Ti films. In bulk Ni-Ti samples, starting with the high temperature $B2$ austenite, the stable martensite $B19'$ forms when cooled to low temperatures. Prior to the formation of $B19'$, the $B2$ austenite may transform into the metastable R -phase martensite, resulting in a two-step transformation sequence

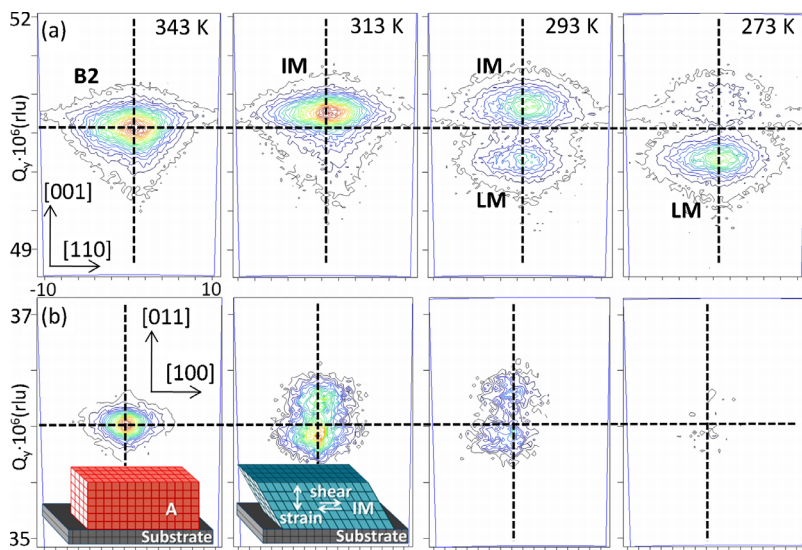


FIG. 3. (Color online) Temperature dependent RSM scans measured (a) around $B2(002)$, and (b) around $B2(011)$ on the $\text{Ni}_{46}\text{Ti}_{54}$ film. Dashed lines are guides to the eye marking the original position of the austenite reflection. Inset figures schematically illustrate the austenite and one variant of the sheared IM structure.

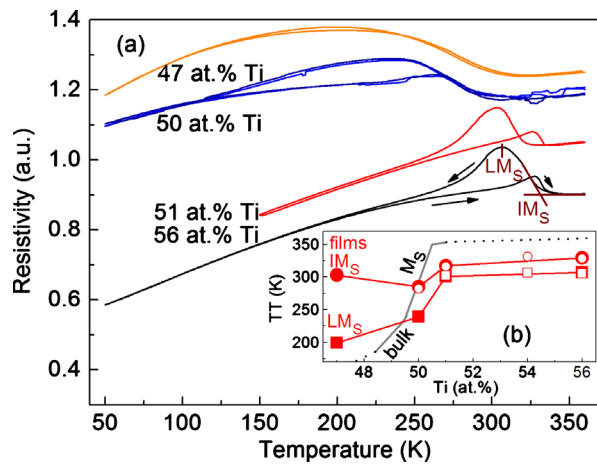


FIG. 4. (Color online) (a) Temperature dependent resistivity of various Ti contents. For 56 at. % Ti, the extraction of transformation start temperatures is shown. (b) Transformation temperatures (TT) obtained from resistivity (solid symbols) and XRD (open symbols), plus the reported $B19'$ martensite start temperature for bulk (M_S , solid gray line) (Refs. 13 and 14) M_S is extrapolated to higher and lower Ti contents by dotted lines.

$B2 \rightarrow R \rightarrow B19'$.³ Zhang and Sehitoglu⁹ observed that the habit planes of the $B2 \rightarrow R$ transformation are close to the $B2(001)$ plane. In addition to the various soft phonon modes in $B2$,¹⁰ the stress stabilized monoclinic distortion angle β of $B19'$ (Ref. 11) gives rise to flexibility in the structure formation in the vicinity of transformation. In the present films, the $B2$ austenite is tetragonally distorted due to the epitaxial lattice mismatch. Despite the distortion, a two step, reversible martensitic phase transformation $B2 \rightarrow IM \rightarrow LM$ is observed, similar to the $B2 \rightarrow R \rightarrow B19'$ sequence in bulk. The metastability of IM suggests that this phase is R -phase related. LM exhibits a XRD peak close to bulk $B19'(022)$ ($2\theta=60.35^\circ$),¹² suggesting that LM could be $B19'$ related. The formation of bulk $B19'(022)$ martensite would, however, require significant lattice distortion at the substrate interface, which is not observed. The present data do not appear to be consistent with a body centered orthorhombic martensite structure.¹¹

For comparison of transformation temperatures in films and bulk, M_S of $B19'$ in bulk Ni-Ti has been added to Fig. 4(b).^{13,14} Though the general trends of M_S and LM_S are similar, LM_S is found to decrease with decreasing Ti content over a wider composition range. For compositions with ≥ 50 at. % Ti both IM_S and LM_S are significantly lower than M_S , indicating that the austenite is preferably stabilized over

the martensites by the symmetry of the MgO substrate interface.

The transformation of the films without tilts of the normal lattice vectors indicates that in-plane transformation strains are suppressed by the substrate.⁷ It is suggested that shearing parallel to the film plane occurs, resulting in the lattice strains being limited to the out-of-plane direction. This mechanism is supported by the reflection splitting upon IM variant formation observed in RSM scans and allows retaining the coherence at interfaces. The resulting low energy of phase boundaries explains the easy initiation of martensitic phase transformations. The substrate plane and the habit plane of this transformation are aligned in parallel. While transformations with inclined habit planes tend to leave residual austenite behind,^{7,15} this specific geometry enables complete and fast martensite transformation in thin films. Though similarities to the $B2 \rightarrow R \rightarrow B19'$ phase sequence are observed in the present films, it is suggested that the structure of the martensites is different from bulk.

We thank J. L. Hall, R. Liptak, and L. Feigl for fruitful discussions. This work was funded by ARO-MURI Grant No. W911NF-07-1-0410. The MRL Central Facilities are supported by the MRSEC Program of the NSF; a member of the NSF-funded Materials Research Facilities Network.

- ¹M. Kohl, *Shape Memory Actuators* (Springer Berlin, Heidelberg, 2004).
- ²K. Bhattacharya, S. Conti, G. Zanzotto, and J. Zimmer, *Nature (London)* **428**, 55 (2004).
- ³K. Otsuka and X. Ren, *Prog. Mater. Sci.* **50**, 511 (2005).
- ⁴H.-J. Lee and A. G. Ramirez, *Appl. Phys. Lett.* **85**, 1146 (2004).
- ⁵R. M. S. Martins, N. Schell, M. Beckers, R. J. C. Silva, K. K. Mahesh, and F. M. Braz Fernandes, *Mater. Sci. Eng., A* **481–482**, 626 (2008).
- ⁶B. Winzek, S. Schmitz, H. Rumpf, T. Sterzl, R. Hassdorf, S. Thienhaus, J. Feydt, M. Moske, and E. Quandt, *Mater. Sci. Eng., A* **378**, 40 (2004).
- ⁷J. Buschbeck, R. Niemann, O. Heczko, M. Thomas, L. Schultz, and S. Fähler, *Acta Mater.* **57**, 2516 (2009).
- ⁸J. W. Dong, J. Q. Xie, J. Lu, C. Adelman, C. J. Palmström, J. Cui, Q. Pan, T. W. Shield, R. D. James, and S. McKernan, *J. Appl. Phys.* **95**, 2593 (2004).
- ⁹X. Zhang and H. Sehitoglu, *Mater. Sci. Eng., A* **374**, 292 (2004).
- ¹⁰X. Y. Huang, C. Bungaro, V. Godlevsky, and K. M. Rabe, *Phys. Rev. B* **65**, 014108 (2001).
- ¹¹X. Y. Huang, G. J. Ackland, and K. M. Rabe, *Nature Mater.* **2**, 307 (2003).
- ¹²Y. Kudoh, M. Tokonami, S. Miyazaki, and K. Otsuka, *Acta Metall.* **33**, 2049 (1985).
- ¹³W. J. Moberly and O. Mercier, *Phys. Metal. Mater. Sci.* **10**, 387 (1979).
- ¹⁴S. Miyazaki, Y. Igo, and K. Otsuka, *Acta Metall.* **34**, 2045 (1986).
- ¹⁵J. Buschbeck, S. Hamann, A. Ludwig, B. Holzapfel, L. Schultz, and S. Fähler, *J. Appl. Phys.* **107**, 113919 (2010).